Colloid and Polymer Science (2019) 297:95–105
https://doi.org/10.1007/s00396-018-4445-1

ORIGINAL CONTRIBUTION

# Enhanced shear thickening of polystyrene-poly(acrylamide) and polystyrene-poly(HEMA) particles

Hoon Soo Son[1] · Kyoung Ho Kim[1] · Joo Hyun Song[1,2] · Wonjoo Lee[2] · Jun Hyeong Kim[3] · Kwan Han Yoon[3] · Young Sil Lee[4] · Hyun-jong Paik[1]

Received: 11 September 2018 / Revised: 18 November 2018 / Accepted: 19 November 2018 / Published online: 24 November 2018


## Abstract

Shear thickening (ST) refers to the drastic increment of viscosity that occurs when a high shear force is applied to certain concentrated colloidal suspensions. The hydrocluster mechanism for ST indicates that inter-particle interaction is important for ST behavior. Therefore, we prepared polystyrene particles with polyacrylamide particles (PS-PAAm particles) to control inter-particle interactions. Colloidal suspensions of polystyrene-poly(2-hydroxyethyl methacrylate) (PS-PHEMA) particles in ethylene glycol were prepared and shown to exhibit strong ST behavior. The effect of PS-PAAm particles on the ST behavior of a PS-PHEMA particle colloidal suspension was investigated; ST behavior of shear thickening fluids (STFs) was controlled by doping different amounts of PS-PAAm particles. We suggested inter-particle interaction was enhanced by abundant hydrogen-bonding donor groups in PS-PAAm particles. Based on this study, the applicability of STF can be increased through the STF fabrication exhibiting desired ST behavior. Also, this study will help to understand fundamental ST mechanism.

**Keywords** Shear thickening · Colloidal suspension · Functionalized polymer particle · Surfactant-free emulsion polymerization

## Introduction

Shear thickening (ST) behavior is a type of non-Newtonian behavior of a concentrated colloidal suspension. The viscosity of a shear thickening fluid (STF) abruptly increases under a high applied shear rate or shear stress, potentially by several orders of magnitude [1, 2]. Shear thickening behavior is a reversible phenomenon, i.e., the viscosity returns to the initial state when the shear stress is removed [3, 4]. Materials exhibiting ST behavior have been used in body armor [5], shock absorbers [6, 7], and damping and control devices [8, 9] because they are flexible when there is no applied shear stress, but rapidly harden at the critical shear rate when the viscosity sharply increases.

The reason for ST behavior is not fully understood, but the "hydrocluster" theory has been accepted as the most probable mechanism. The hydrocluster theory asserts that ST behavior arises from the formation of shear-induced particle clusters by short-range lubrication hydrodynamic forces [10]. Brady and Bossis first proposed a hydrocluster mechanism for particle agglomerates formed by shear using Stokesian dynamics simulations [11]. Rheo-optical experiments [12, 13], stress-jump rheological measurements [14], and neutron scattering [15, 16] have also been used to study this mechanism. Recently, the frictional contact interactions between particles to explain the shear thickening response are actively introduced. Seto et al. found that the critical volume fraction for the shear thickening is a function of the particle friction coefficient using particle-scale simulation [17]. Hsu et al. demonstrated the effect of particle roughness on the shear thickening transition using model silica colloidal suspension. They found that rougher surfaces of the particle contributed to the enhancement of the shear thickening effect because of interlocking of asperities [18]. Notably, Cheng et al. confirmed and

✉ Young Sil Lee
youngsil@kumoh.ac.kr

✉ Hyun-jong Paik
hpaik@pusan.ac.kr

[1] Department of Polymer Science and Engineering, Pusan National University, Busan 46241, South Korea

[2] Center for Chemical Industry Development, Korea Research Institute of Chemical Technology, Daejeon 44412, South Korea

[3] Department of Chemical Engineering, Kumoh National Institute of Technology, Gumi 39177, South Korea

[4] Industry-Academic Cooperation, Kumoh National Institute of Technology, Gumi 39177, South Korea

visualized ST behavior, due to the formation of hydroclusters via hydrodynamic lubrication forces, by combining fast confocal microscopy with simultaneous force measurements [19]. They also demonstrated that the order–disorder transition affects ST behavior but is not dominant.

Shear thickening behavior is influenced by particle parameters such as volume fraction [20], shape [21], size [22], size [23] distribution, and inter-particle interactions [24]. Among these, inter-particle interactions can be enhanced by introducing hydrogen bonds as secondary bonds on the particle surface. Inter-particle hydrogen bonding has been used to explain the mechanism of ST behavior [25, 26]. Suspensions of particles having functional groups capable of hydrogen bonding on their surfaces exhibit stronger ST behavior than those having no hydrogen-bondable functional groups [27]. Zhou et al. did not observe ST behavior for a suspension of silica particles whose surface hydroxyl groups were removed by a thermal treatment [28]. These results indicate that the presence of functional groups capable of hydrogen bonding on a particle surface has a significant effect on the ST behavior of the fluid. Jiang et al. observed high ST behavior at low volume fractions for polydopamine coated with silica particles having abundant surface hydroxyl groups [29]. The rheological properties of STFs can thus be changed using various approaches to control inter-particle interactions.

We previously reported strong ST behavior for suspensions of polystyrene-poly(2-hydroxyethyl methacrylate) particles (PS-PHEMA particles) [30]. The behavior was attributed to strong inter-particle interactions due to abundant hydrogen-bondable groups on the surface of the PS-PHEMA particles. In this work, the rheological properties of a mixed suspension of polystyrene-polyacrylamide particles (PS-PAAm particles) and PS-PHEMA particles were studied. The ST behavior was significantly enhanced compared with that of the suspension of only PS-PHEMA particles. These results are attributed to hydrogen bonding between donor groups present on the PAAm backbone with acceptor groups on the PS-PHEMA particles.

## Experimental section

### Materials

2-Hydroxyethyl methacrylate (HEMA) (Sigma, 97.0%), styrene (St; Daejung, > 99%,) and divinylbenzene (DVB; Sigma, 80%) had their inhibitors removed by passing through basic alumina. Acrylamide (AAm; Sigma, > 99%) was used as-received. Potassium persulfate (KPS; Sigma, > 99%) was recrystallized from water to remove impurities. Triply-distilled water was used in this work.

### Preparation of the polymer particles

PS-PAAm particles were synthesized via surfactant-free emulsion polymerization from AAm and St, with DVB as the cross-linker and KPS as the initiator. The synthesis was conducted in a 1000-mL round-bottomed flask. Styrene (48.16 mL, 0.42 mol), AAm (2.99 g, 0.042 mol), DVB (4.79 mL, 0.034 mol), and triply-distilled water (580 mL) were added to the flask and deoxygenated by sparging with $N_2$ for at least 20 min. Polymerization was done under $N_2$ for 24 h, after which the product was obtained by centrifugation. The final product was dried overnight in a vacuum oven at 30 °C. The PS-PHEMA particles were synthesized similarly, as described previously [30].

### The preparation of PS-PHEMA particles with PS-PAAm particle suspension

The STFs were prepared as follows. A fixed amount of particles was added directly to EG. The mixture was ball-milled to obtain a uniform suspension, with the progress checked every 12 h. The final particle suspension was attained when no large aggregates were visually identified in the suspension; it was then degassed by sonicating for 30 min.

### Characterization

Dynamic light scattering (DLS) data were obtained using a 90Plus device (Brookhaven Instruments). Field emission scanning electron microscope (20 kV) images were acquired with a Supra 25 instrument (Carl Zeiss). Transmission electron microscopy (TEM) images were obtained using a H-7600 instrument (Hitachi). Infrared spectra were recorded over 4000–650 $cm^{-1}$ using a 6700 Fourier transform infrared (FT-IR) spectrometer (Nicolet) using KBr pellets. X-ray photoelectron spectra (XPS) were obtained using an AR-XPS system (Theta Probe). Zeta potential data were acquired with a Zetasizer Nano-ZS (Malvern Panalytical).

### Rheological measurements

A rotational rheometer (Discovery HR-2; TA Instruments) was used to measure the rheological properties of the colloidal suspensions. A cone-and-plate geometry (plate diameter 40 mm; cone angle 2°) was used. The steady-state shear viscosity of samples was measured at 25 °C. Any loading effect was removed by pre-shearing at 1 $s^{-1}$ for 5 min. Each experiment was repeated five times for each condition.

## Results and discussion

### Synthesis of the PS-PHEMA particles and PS-PAAm particles

The PS-PHEMA particles and PS-PAAm particles were synthesized using surfactant-free emulsion polymerization. The reaction was initiated in two phases because of the solubility difference between the hydrophobic monomer, i.e., St, and the hydrophilic monomers, i.e., AAm and HEMA. Because the water-soluble initiator KPS was used, the monomers dissolved in the water phase were preferentially polymerized. Thereafter, as the concentration of the water-soluble monomer decreased, St was preferentially polymerized. As polymerization proceeded, the more hydrophilic PAAm and PHEMA were deposited on the particle surfaces depending on their affinity to water. The hydrophobic PS formed the core. Particles were synthesized in this manner and characterized by DLS, SEM, and TEM (Fig. 1). DLS indicated particle diameters of ca. 390 nm for the PS-PHEMA particles and ca. 410 nm for the PS-PAAm particles; each had a narrow size distribution. Both types of particles had rough surfaces characteristic of particles synthesized by surfactant-free emulsion polymerization [31]. TEM imaging indicated a lower electron density at the particle surface than at the core and confirmed particle formation mechanism which we suggested.

The constituents of the particles were confirmed by FT-IR (Fig. 2). Since both PS-PHEMA particles and PS-PAAm particles contain PS, they show an aromatic overtone peak at ca. 1900 $cm^{-1}$ and an aromatic C=C stretching doublet at ca. 1475 $cm^{-1}$. However, the different shell compositions resulted in distinct peaks. The PS-PAAm particles exhibited a secondary amine group (–NH) stretching peak at ca. 3400 $cm^{-1}$, while the PS-HEMA particles exhibited a broad hydroxyl group (–OH) stretching peak. The stretching peak of the carbonyl group (C=O) also appeared at different wavenumbers: PS-PAAm particles show this at 1690 $cm^{-1}$ for the amide C=O peak, while an ester C=O peak appears at 1735 $cm^{-1}$ for PS-PHEMA particles. The N–H bending peaks of PS-PAAm particles appeared at ca. 1600 $cm^{-1}$, hiding the aromatic double bond (C=C) stretching peak. For the PS-PHEMA particles, there was no overlapping peak, and an aromatic C=C stretching peak was observed. The FT-IR results could readily differentiate the PS-PHEMA particles and PS-PAAm particles.

The XPS spectroscopy was used to analyze the surface of the synthesized particles. Since both particles are composed of organic materials, strong C1s peaks were clearly observed in the spectra of PS-PHEMA particles and PS-PAAm particles. The O1s peaks appearing in both were stronger for PS-PHEMA particles because of its higher oxygen content (Fig. 3b). Considering oxygen-containing functional groups,

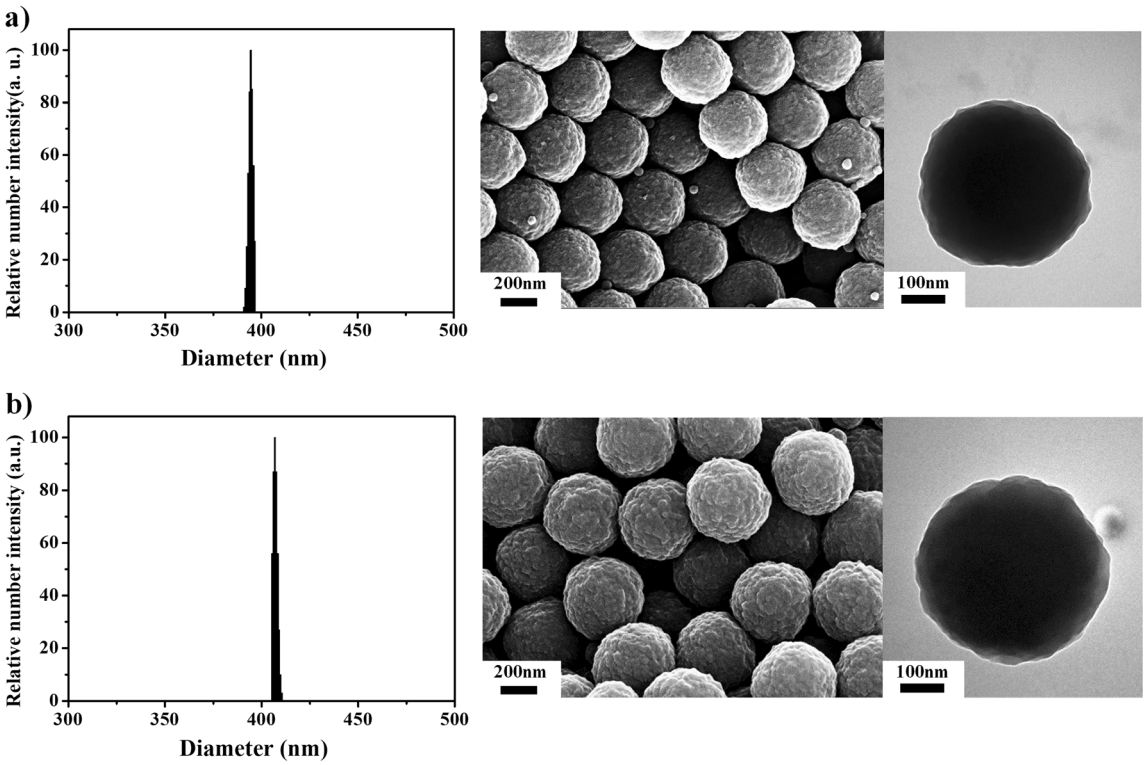


**Fig. 1** Dynamic light scattering, scanning electron microscopy, and transmission electron microscopy images of **a** PS-PHEMA particles and **b** PS-PAAm particles

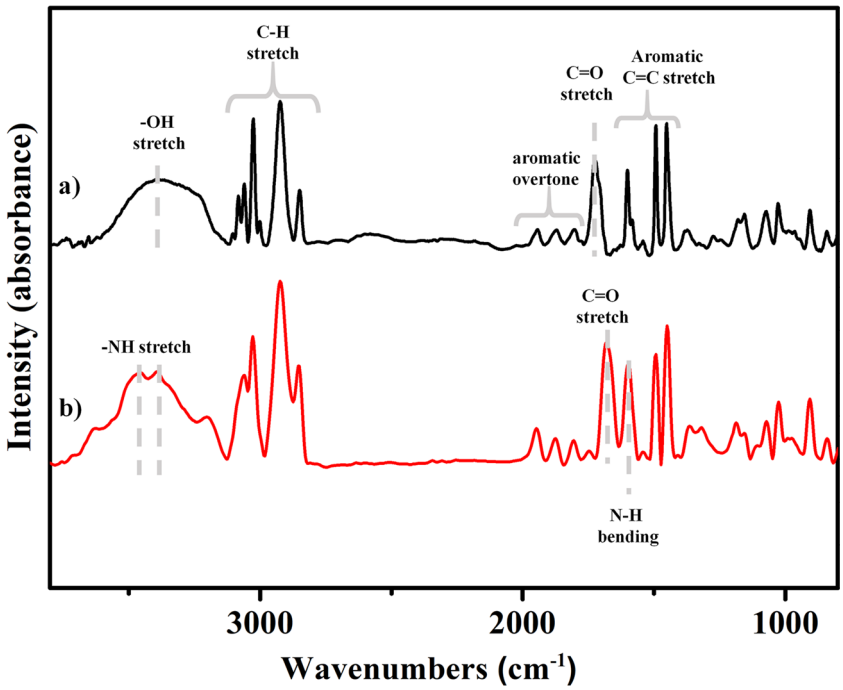


**Fig. 2** Fourier transform infrared spectra of (a) PS-PHEMA particles and (b) PS-PAAm particles

PS-PHEMA contains ether (C–O–C) and hydroxyl (–OH) linkages while PS-PAAm particles contain only carbonyl groups (C=O). The distinct N1s peak observed for the PS-PAAm particles is attributed to the polyacrylamide amine (–NH) group on the surface of the PS-PAAm (Fig. 3a). These XPS results indicate that PHEMA or PAAm was located on the particle surfaces.

The surface charge of the PS-PHEMA particles and PS-PAAm particles was measured in terms of zeta potential (Fig. 4). Since both particles were synthesized using anionic initiator KPS, they had a negative charge on the surface. The zeta potential values of PS-PHEMA and PS-PAAm particles were −24.2 mV and −21.5 mV, respectively. These results indicate that the sulfate group at the end of the polymer is present and that the polymer particles have colloidal stability due to negative charge during the synthesis process. Also, we checked the zeta potential value of the PS-PAAm particle and PS-PHEMA particle mixture (PS-PHEMA particles:PS-

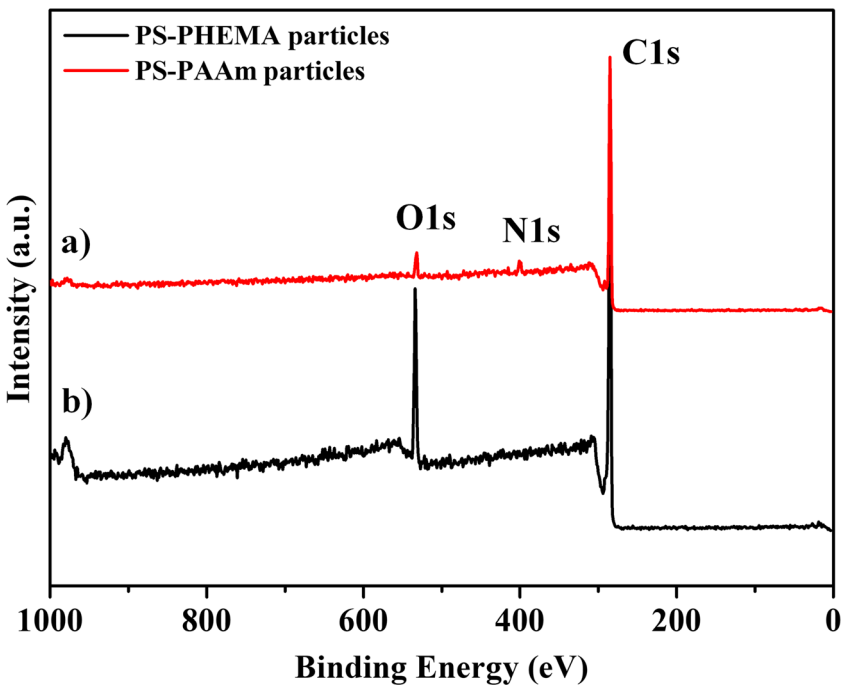


**Fig. 3** XPS spectra of (a) PS-PAAm particles and (b) PS-PHEMA particles

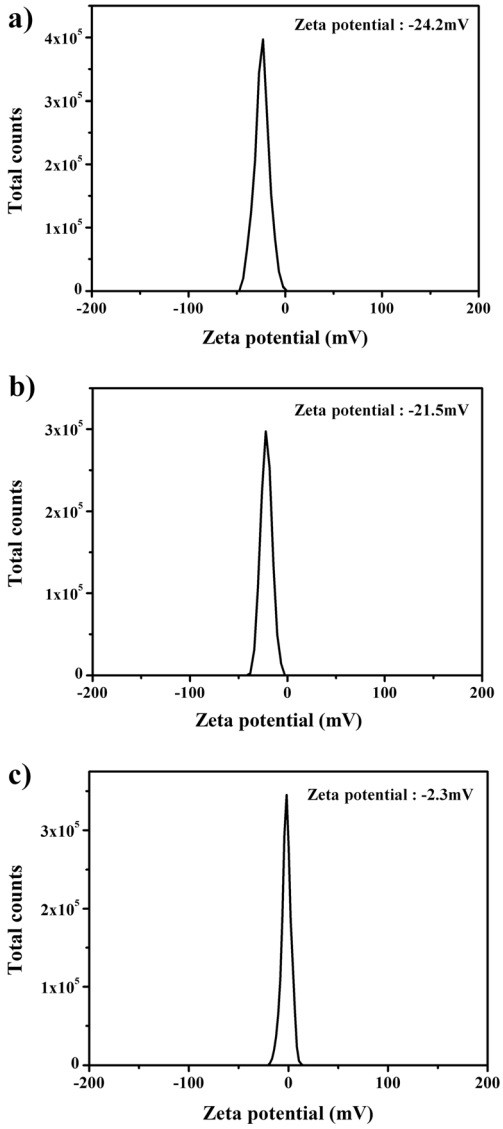


**Fig. 4** Surface zeta potential values of **a** PS-PAAm particles, **b** PS-PHEMA particles, and **c** PS-PAAm particle and PS-PHEMA particle mixture

PAAm particles = 25:1). We could find lower zeta potential value of − 2.3 mV than in only PS-PHEMA or PS-PAAm particles. Based on this result, we suggest that enhancement of inter-particle interaction by PS-PAAm particle decreased particle stability.

## Rheological properties of PS-PHEMA particle and PS-PAAm particle suspensions

PS-PHEMA particle and PS-PAAm particle suspensions were prepared by directly adding the particles to ethylene glycol (EG) and treating the mixtures in a ball mill. The PS-PHEMA particle suspension exhibited a low initial viscosity at low shear rates due to medium–particle interactions between the abundant hydrogen-bondable groups on the PS-PHEMA particle surfaces and repulsive forces from the charged surfaces. However, strong ST behavior was apparent at high shear rates due to inter-particle interactions between the hydrogen-bondable groups on the particle surfaces at small inter-particle distances. For the 50 wt% PS-PHEMA particle suspension, the critical shear rate and maximum viscosity were 75.0 $s^{-1}$ and 35.6 Pa s, respectively, and 7.5 $s^{-1}$ and 145.3 Pa s for the 52 wt% PS-PHEMA particle suspension. Figure 5 shows that the ST behavior was strongly influenced by the particle concentration. The critical shear rate decreased, and the maximum viscosity increased, with increasing particle concentration. With increasing particle mass fraction, the mean distance between particles becomes smaller and particle cluster formation due to hydrodynamic forces is facilitated [32].

However, the 50 wt% PS-PAAm particle suspension only displayed shear thinning, not ST, behavior (Fig. 6). A very high viscosity of 476.2 Pa s was observed at low shear rate, and no increment of viscosity was evident with increasing shear rate until 1000 1/s. This result suggested that particle clusters were present in the absence of shear loading. Previous research indicated that ST behavior does not occur when particle interactions become too strong and there is pronounced flocculation [33]. Our results are likely due to flocculation resulting from strong inter-particle interactions between strongly hydrogen-bonded PS-PAAm particles.

As, the PS-PAAm particles with no ST behavior were mixed with PS-PHEMA particles displaying well-behaved ST behavior, the ST behavior was substantially improved. The weight fraction of the two particles was fixed between 50 and 52 wt%, and the PS-PAAm particles were added at different compounding ratios (PS-PHEMA/PS-PAAm = 25/1, 50/1, 100/1). In both cases, as the PS-PAAm particle ratio increased, there was a decrease in the ST critical shear rate and increase in the initial viscosity and maximum viscosity. For example, PS-PHEMA to PS-PAAm ratio at 25/1 with a weight fraction of 50 wt%, the maximum viscosity increased 2.0-fold from 35.62 to 71.69 Pa s and the critical shear rate for shear thickening (ST) decreased from 56.23 to 31.62 $s^{-1}$. For the 52 wt% case, the maximum viscosity increased 5.0-fold from 145.29 to 729.76 Pa s and the critical shear rate for ST decreased from 4.22 to 2.91 $s^{-1}$ (Fig. 7). Details of the other particle ratios are shown in Table 1. Notably, stronger ST behavior was observed with the higher particle weight fraction case.

In Fig. 7, the hydrogen-bonding enhancement of PS-PAAm particles influences the initial viscosity and shear thinning effect. As the content of PS-PAAm particles increases, the initial viscosity increases and shear thinning behavior also occurs rapidly. Particularly, when PS-PHEMA particle:PS-PAAm particle = 25:1 and particle weight percent = 52 wt% condition, sudden change appeared. This result is due to agglomeration already formed at low shear rate due to inter-

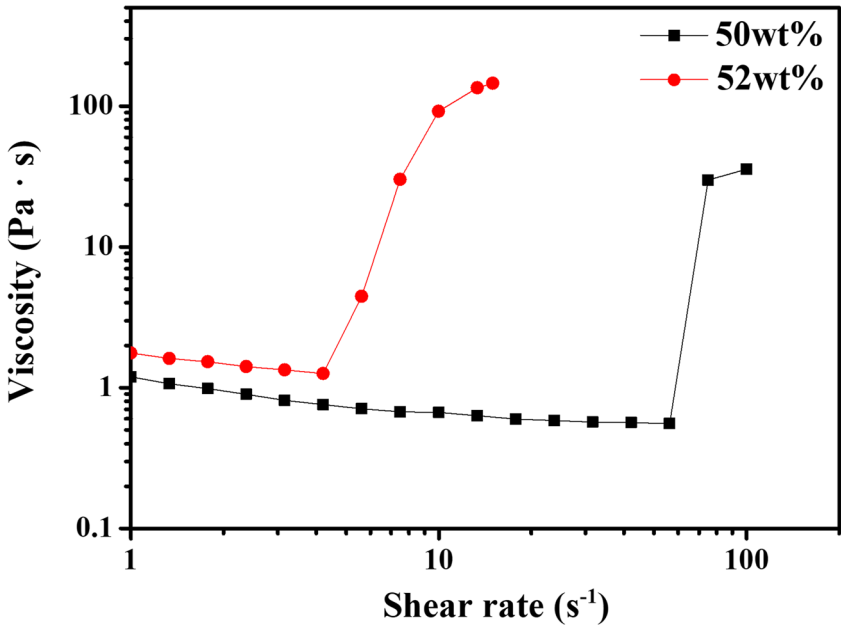


**Fig. 5** Rheological data of PS-PHEMA particle suspension (black dot line 50 wt%, red dot line 52 wt%)

particle hydrogen-bonding enhancement. The viscosity of the suspension increases as the concentration of the particle increases, and diverges near a maximum particle packing fraction which is 0.64 for random closed packing [34]. So, the viscosity is dramatically increased at higher concentration by a small change of concentration of the particle. If the agglomeration is already formed, the viscosity is relatively high because of the increase of the hydrodynamic volume of the particle agglomerate compare with the one of the individual particle, and the agglomeration is removed by the shear, resulting in a rapid shear thinning phenomenon. Enhancement of the viscosity at low shear rate increases even more as the concentration and number of agglomerate increase.

The ST behavior of the mixed PS-PAAm particle and PS-PHEMA particle suspension under cyclic loading was investigated to confirm the reversibility of the ST behavior. Figure 8 shows the change in viscosity of the 50 wt% sample as the shear rate ascended and descended. With increasing shear rate, the viscosity decreased slightly at low shear rates but increased steeply at the critical shear rate. With descending shear rate, the viscosity returned from its high value to the initial one and showed a similar critical shear rate to that observed with

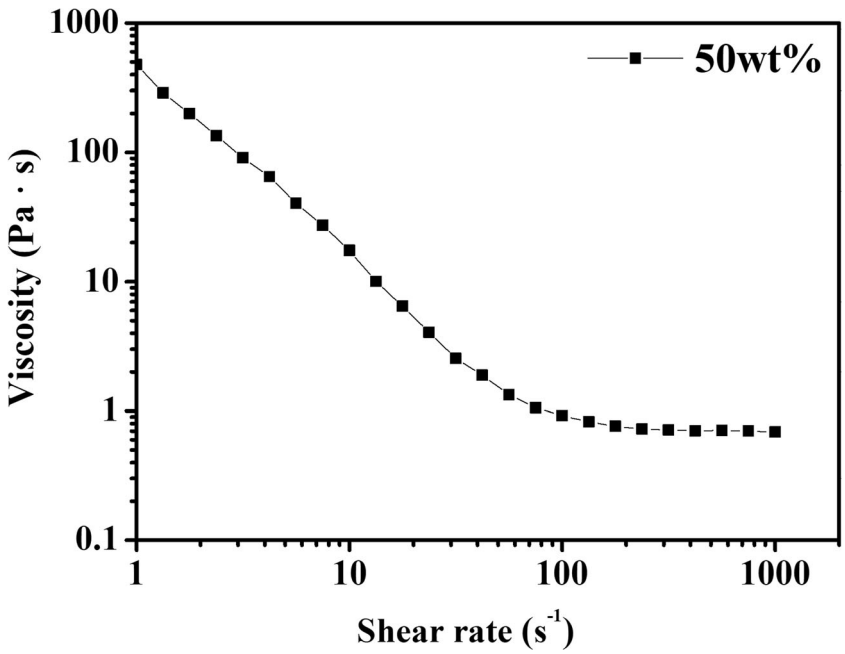


**Fig. 6** Rheological data of PS-PAAm particle suspension (50 wt%)

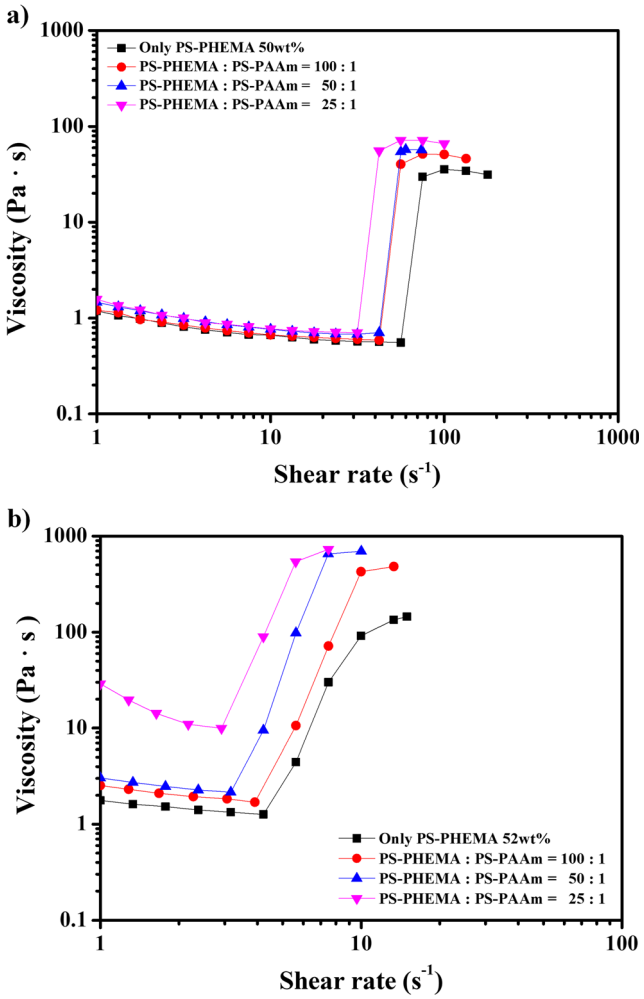


**Fig. 7** Rheological data of PS-PHEMA and PS-PAAm particle mixed suspension. **a** 50 wt%. **b** 52 wt%

increasing shear rate. This result implies that the hydroclusters that formed at high shear rates collapsed due to a decrease in hydrodynamic lubrication forces as the shear rate decreased, and finally returned to a well-dispersed state of suspension. The combination of PS-PAAm particles and PS-PHEMA particles thus provided a colloidal suspension having an improved and reversible ST behavior. This would be of great interest for industrial applications such as flexible body armor, shock absorbers, and damping devices.

## Mechanism of enhancing ST behavior

The mixed suspension of PS-PHEMA particles and PS-PAAm particles showed higher ST behavior than the suspension containing only PS-PHEMA particles. We suggest a hypothesis for these results: the PS-PAAm particles enhanced inter-particle interactions via groups other than hydrogen-bond donor groups of the PS-PHEMA. For HEMA located on the surface of the PS-PHEMA particles, there is one hydrogen-bond donor in the hydroxyl group (–OH) but many hydrogen-bond acceptors among the ester (–COO–) and hydroxyl (–O:) groups. Therefore, there are likely residual hydrogen-bond acceptor groups that cannot hydrogen bond because there are more hydrogen-bond acceptors than hydrogen-bond donors in the interactions between PS-PHEMA particles. On the other hand, concerning AAm on the surface of the PS-PAAm particles, there are two hydrogen-bond donors and a relatively strong hydrogen-bond acceptor (–N:) in the amine group ($–NH_2$). Scheme 1 shows the PS-PHEMA particles and PS-PAAm particles. The PS-PAAm particles with abundant hydrogen-bond donors are located between the PS-PHEMA particles, filling the residual hydrogen-bond acceptors of PS-PHEMA particles and thereby enhancing inter-particle interactions. This enhancement improved the ST behavior because particle clusters formed more easily with the applied shear stress (or shear rate).

According to the hydrocluster mechanism, in the absence of a shear stress (or shear rate), the equilibrium state of random collisions due to Brownian motion of well-dispersed particles is maintained (Scheme 2(a)). When an external shear stress (or shear rate) is applied, the particles are oriented in the shear flow direction and the viscosity of the suspension decreases; this is called shear thinning (Scheme 2(b)). When the shear rate reaches the critical shear rate, the hydrodynamic

**Table 1** Detailed values of ST behavior in STFs based on PS-PHEMA particles and PS-PAAm particles

| Weight fraction (wt%) | [a]Particle ratio | Initial viscosity (Pa s) | Critical shear rate ($s^{-1}$) | Maximum viscosity (Pa s) |
|---|---|---|---|---|
| 50 | Only PS-PHEMA particle | 1.19 | 56.23 | 35.62 |
| | 100/1 | 1.21 | 42.17 | 51.69 |
| | 50/1 | 1.47 | 40.29 | 57.22 |
| | 25/1 | 1.57 | 31.62 | 71.69 |
| 52 | Only PS-PHEMA particle | 1.77 | 4.22 | 145.29 |
| | 100/1 | 2.63 | 3.92 | 481.78 |
| | 50/1 | 3.03 | 3.16 | 697.05 |
| | 25/1 | 28.96 | 2.91 | 726.76 |

[a] PS-PHEMA particles/PS-PAAm particles

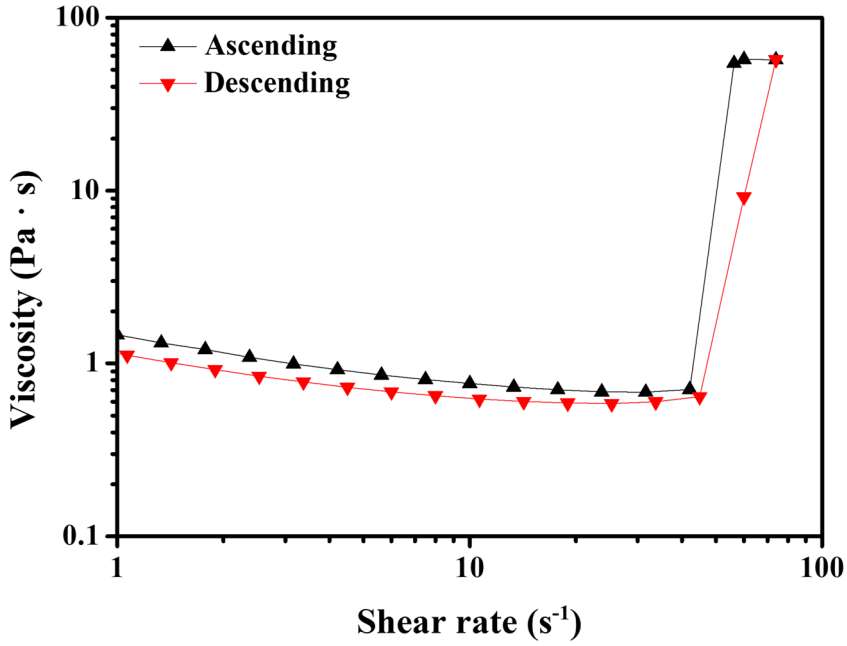


**Fig. 8** Reversible ST behavior of PS-PHEMA particle and PS-PAAm particle suspension (50 wt%, PS-PHEMA particle/PS-PAAm particle = 50/1)

interactions between particles form local clusters. The resultant sharp increase in viscosity is called ST (Scheme 2(c)). Inter-particle interactions greatly influence ST behavior. Hence, physical bonding (van der Waals forces, hydrogen bonds) between particles is generally used to describe the mechanism of ST behavior. When inter-particle interactions are strengthened, hydroclusters can be readily formed by hydrodynamic forces. Thus, enhancing inter-particle interactions at the level of good dispersion leads to higher ST behavior. Enhancement of inter-particle hydrogen bonding by adding PS-PAAm particles resulted in a lower critical shear rate and a higher maximum viscosity. Therefore, in the PS-PAAm particles and PS-PHEMA suspensions, more hydroclusters formed than in the suspension of only PS-PHEMA particles, and the formed hydroclusters were likely larger in the mixed PS-PAAm particles and PS-PHEMA suspension than in the PS-PHEMA particle–only suspension.

In the prepared colloidal suspension, the forces involved in inter-particle interaction include secondary attractive interaction (e.g., van der Waals force, hydrogen bonding) and electrostatic repulsive force. Under critical shear rate, the particles were kept well-dispersed state by making electrostatic repulsive force stronger than secondary attractive interaction. However, when the high shear rate was applied to the colloidal suspension, the distance between the particles became closer due to the physical force, and secondary attractive interaction between the particles greatly affected the rheological properties of the fluid. At this time, because hydrogen bonding is stronger than van der Waals force existed between particles, inter-particle interaction was dominated by hydrogen bonding. A hydrogen bond is the attraction between the lone pair of an electronegative atom and a hydrogen atom that is bonded to either nitrogen, oxygen, or fluorine. Hydrogen bond is described as a strong electrostatic dipole–dipole interaction. It is directional and stronger than van der Waals interaction and produces interatomic distances shorter than van der Waals bond [35, 36]. Therefore, the enhancement of inter-particle interaction by the provision of hydrogen-bonding donors of PS-PAAm particles greatly affects the ST behavior of colloidal suspension. Based on these discussions, our study can help to understand the influence of inter-particle interaction on ST behavior and fundamental mechanism.

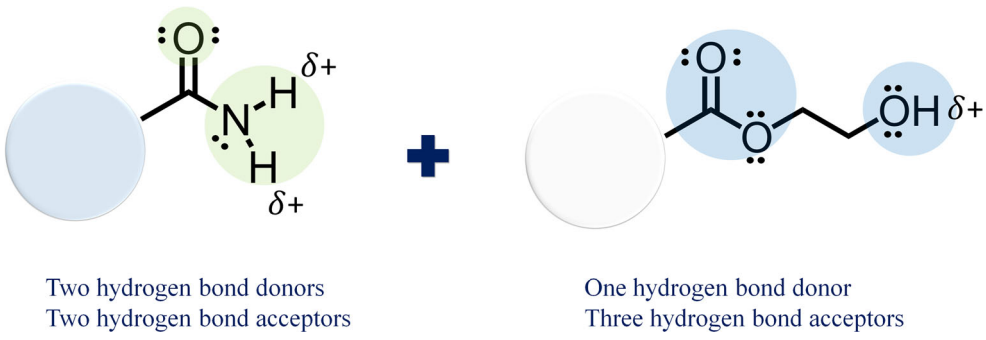


**Scheme 1** Functional groups of the polystyrene-polyacrylamide particles (PS-PAAm particles) and polystyrene-poly(2-hydroxyethyl methacrylate) particles (PS-PHEMA particles)

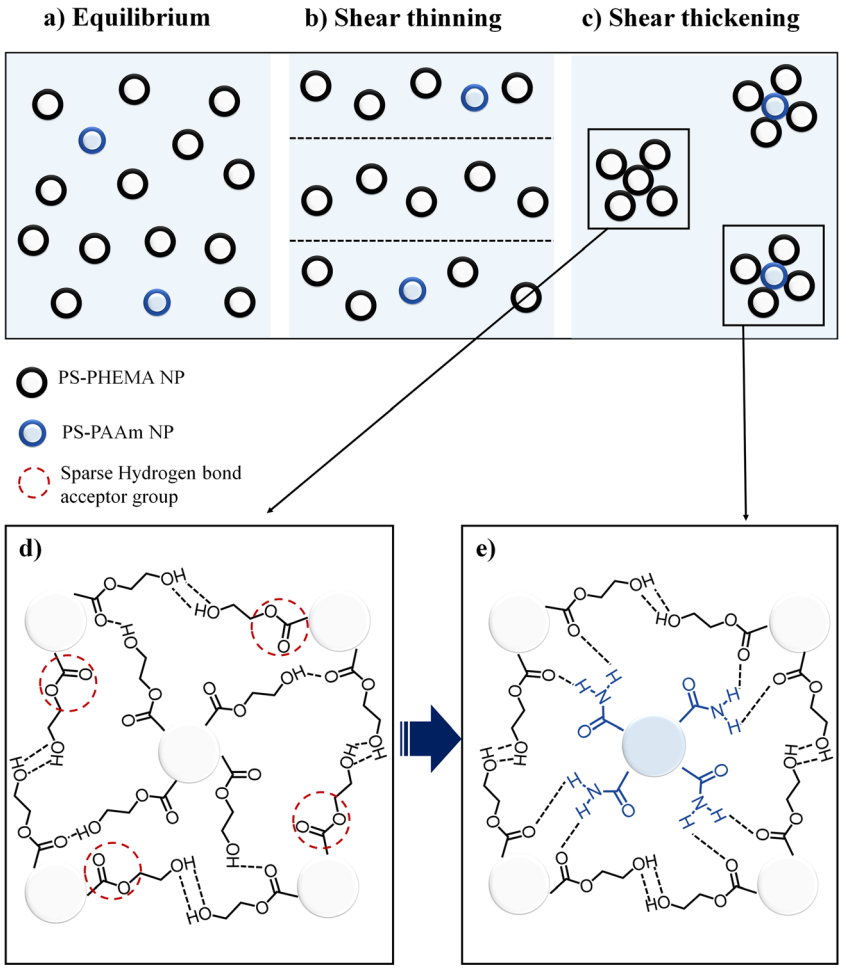


**Scheme 2** Mechanism of enhancing ST behavior

In this work, the weight fraction of dispersed particles was fixed between 50 and 52 wt%. As the particle weight fraction increased, the inter-particle distance diminished, facilitating hydrocluster formation by inter-particle hydrogen bonding. Thus, the effect of PS-PAAm particles on inter-particle interactions was stronger at higher weight fractions. The evidence for this phenomenon is as follows: increment of maximum viscosity and initial viscosity in the STF of the high-particle weight fraction was relatively high. In higher particle weight fractions, the inter-particle interaction by PS-PAAm particles will be stronger because the inter-particle distances decreased and come close to each other.

Recently, Hsu et al. also reported the roughness-dependent tribology effects on discontinuous shear thickening [18]. They showed increasing the surface roughness of the particle enhanced the shear thickening effect and shifted it to both lower the volume fraction of the particle for the shear thickening and shear viscosity at shear thinning region. Both PS-PHEMA and PS-PAAm particles synthesized in this research work have some roughness on the surface as shown in Fig. 1, but PS-PAAm particle is a little bit more rugged than PS-PHEMA particle. The tendency of the lowering of the critical shear rate for the shear thickening and higher maximum viscosity at shear thickening when the content of PS-PAAm was increased is consistent with the report of Hsu et al. But the tendency of the increase of the viscosity at low shear rate as the content of PS-PAAm particles increases is contradictory to their result. Surface roughness and friction mechanism play an important role in the shear thickening behavior of our system because of the rough surfaces of the PS-PHEMA and PS-PAAm particles.

Colloidal suspension shows the continuous shear thickening (CST) at intermediate concentrations of the particles while showing the discontinuous shear thickening (DST) with much higher concentration. It is not easy to explain DST mechanism using only hydrodynamic interaction which includes the order–disorder transition and hydrocluster mechanisms while hydrodynamic interaction is the most important part for CST. In our system, it is difficult to find CST for intermediate concentration of the particles; the suspension shows the shear thinning behavior until it switched to DST. This kind of behavior has been reported by Hsu et al. using different types of the surface of the

particles [18]. For smooth colloids, they show CST behavior for intermediate concentration of particle and display DST at 0.58 of particle volume fraction which is very close to the maximum particle packing fraction. But rough colloids which surface is similar with our polymer particles only show DST behavior without CST. It is explained that for rough particles, the formation of the particle chain occurs as soon as a hydrodynamic lubrication film breaks which is called "stick-slip" frictional contact, while smooth particles experience normal sliding friction.

In this study, as the ratio of PS-PAAm particles increases, the strengthening of the ST behavior increases. These results suggest that the weight fraction of particles with ST behavior can be reduced while controlling the ST behavior through the addition of the other particles. Thus, the combination of PS-PHEMA and PS-PAAm particles makes it possible to lighten the STF. The tailored ST behavior of an STF can be achieved by adjusting the ratio of PS-PHEMA and PS-PAAm particles for a given application.

## Conclusion

Combining PS-PAAm particles with PS-PHEMA particles in a suspension showed improved ST behavior compared with the suspension comprising only PS-PHEMA particles. The PS-PAAm particles and PS-PHEMA particles were synthesized by a surfactant-free emulsion polymerization method. The synthesized particles were directly added to EG and dispersed using a ball mill to produce the STF. The ST behavior of PS-PAAm particles and PS-PHEMA suspensions at low and high weight fractions was measured; they displayed lower critical shear rates and higher maximum viscosities than the PS-PHEMA particle–only suspension having the same weight fraction. This result suggests that the abundant hydrogen-bond donor groups of PS-PAAm particles interacted with the remaining hydrogen-bond acceptor groups that did not hydrogen bond with the PS-PHEMA particles, thereby enhancing inter-particle interactions. The enhancement of ST behavior achieved by enhancing inter-particle interactions, through combing PS-PAAm particles and PS-PHEMA particles, is of interest for industrial applications requiring light-weight STFs.

**Acknowledgements** Assistance in the XPS analysis from the Korea Basic Science Institute (KBSI) Busan Center is acknowledged.

**Funding information** This work was supported by the Industrial Strategic Technology Development Program (Grant Nos. 10063082 and 10070127) funded by the Ministry of Trade, Industry and Energy (MOTIE) of Korea. This research has been performed as a cooperation project of "The development of Sustainable materials technology for Eco-Automobile" and supported by the Korea Research Institute of Chemical Technology (KRICT)

## References

1. Hoffman R (1972) Discontinuous and dilatant viscosity behavior in concentrated suspensions. I. Observation of a flow instability. Trans Soc Rheol 16(1):155–173
2. Hoffman R (1974) Discontinuous and dilatant viscosity behavior in concentrated suspensions. II. Theory and experimental tests. J Colloid Interface Sci 46(3):491–506
3. Barnes H (1989) Shear-thickening ("Dilatancy") in suspensions of nonaggregating solid particles dispersed in Newtonian liquids. J Rheol 33(2):329–366
4. Bender J, Wagner NJ (1996) Reversible shear thickening in monodisperse and bidisperse colloidal dispersions. J Rheol 40(5):899–916
5. Lee YS, Wetzel ED, Wagner NJ (2003) The ballistic impact characteristics of Kevlar® woven fabrics impregnated with a colloidal shear thickening fluid. J Mater Sci 38(13):2825–2833
6. Kang TJ, Kim CY, Hong KH (2012) Rheological behavior of concentrated silica suspension and its application to soft armor. J Appl Polym Sci 124(2):1534–1541
7. Srivastava A, Majumdar A, Butola BS (2011) Improving the impact resistance performance of Kevlar fabrics using silica based shear thickening fluid. Mater Sci Eng A 529:224–229
8. Fischer C, Braun S, Bourban P, Michaud V, Plummer C, Manson JE (2006) Dynamic properties of sandwich structures with integrated shear-thickening fluids. Smart Mater Struct 15(5):1467–1475
9. Zhang X, Li W, Gong X (2008) The rheology of shear thickening fluid (STF) and the dynamic performance of an STF-filled damper. Smart Mater Struct 17(3):035027
10. Wagner NJ, Brady JF (2009) Shear thickening in colloidal dispersions. Phys Today 62(10):27–32
11. Brady JF, Bossis G (1985) The rheology of concentrated suspensions of spheres in simple shear flow by numerical simulation. J Fluid Mech 155:105–129
12. Kishbaugh A, McHugh A (1993) A rheo-optical study of shear-thickening and structure formation in polymer solutions. Part I: experimental. Rheol Acta 32(1):9–24
13. Kishbaugh A, McHugh A (1993) A rheo-optical study of shear-thickening and structure formation in polymer solutions. Part II: light scattering analysis. Rheol Acta 32(2):115–131
14. O'Brie VT, Mackay ME (2000) Stress components and shear thickening of concentrated hard sphere suspensions. Langmuir 16(21): 7931–7938
15. Maranzano BJ, Wagner NJ (2002) Flow-small angle neutron scattering measurements of colloidal dispersion microstructure evolution through the shear thickening transition. J Chem Phys 117(22): 10291–10302
16. Lee YS, Wagner NJ (2006) Rheological properties and small-angle neutron scattering of a shear thickening, nanoparticle dispersion at high shear rates. Ind Eng Chem Res 45(21):7015–7024
17. Seto R, Mari R, Morris JF, Denn MM (2013) Discontinuous shear thickening of frictional hard-sphere suspensions. Phys Rev Lett 111(21):218301
18. Hsu C-P, Ramakrishna SN, Zanini M, Spencer ND, Isa L (2018) Roughness-dependent tribology effects on discontinuous shear thickening. Proc Natl Acad Sci 201801066
19. Cheng X, McCoy JH, Israelachvili JN, Cohen I (2011) Imaging the microscopic structure of shear thinning and thickening colloidal suspensions. Science 333(6047):1276–1279
20. Liu X-Q, Bao R-Y, Wu X-J, Yang W, Xie B-H, Yang M-B (2015) Temperature induced gelation transition of a fumed silica/PEG shear thickening fluid. RSC Adv 5(24):18367–18374
21. Srivastava A, Majumdar A, Butola B (2012) Improving the impact resistance of textile structures by using shear thickening fluids: a review. Critical reviews in solid state and materials. Sciences 37(2): 115–129

22. Lee B-W, Kim I-J, Kim C-G (2009) The influence of the particle size of silica on the ballistic performance of fabrics impregnated with silica colloidal suspension. J Compos Mater 43(23):2679–2698
23. Olhero S, Ferreira J (2004) Influence of particle size distribution on rheology and particle packing of silica-based suspensions. Powder Technol 139(1):69–75
24. Maranzano BJ, Wagner NJ (2001) The effects of inter-particle interactions and particle size on reversible shear thickening: hard-sphere colloidal dispersions. J Rheol 45(5):1205–1222
25. Chu B, Brady AT, Mannhalter BD, Salem DR (2014) Effect of silica particle surface chemistry on the shear thickening behaviour of concentrated colloidal suspensions. J Phys D Appl Phys 47(33): 335302
26. Warren J, Offenberger S, Toghiani H, Pittman Jr CU, Lacy TE, Kundu S (2015) Effect of temperature on the shear-thickening behavior of fumed silica suspensions. ACS Appl Mater Interfaces 7(33):18650–18661
27. Jiang W, Ye F, He Q, Gong X, Feng J, Lu L, Xuan S (2014) Study of the particles' structure dependent rheological behavior for polymer nanospheres based shear thickening fluid. J Colloid Interface Sci 413:8–16
28. Yang W, Wu Y, Pei X, Zhou F, Xue Q (2017) Contribution of surface chemistry to the shear thickening of silica nanoparticle suspensions. Langmuir 33(4):1037–1042
29. Liu M, Jiang W, Chen Q, Wang S, Mao Y, Gong X, Leung KC-F, Tian J, Wang H, Xuan S (2016) A facile one-step method to synthesize SiO 2@ polydopamine core–shell nanospheres for shear thickening fluid. RSC Adv 6(35):29279–29287
30. Son HS, Kim KH, Kim JH, Yoon KH, Lee YS, Paik H-j (2018) High-performance shear thickening of polystyrene particles with poly (HEMA). Colloid Polym Sci 296(9):1591–1598
31. Dobrowolska ME, van Esch JH, Koper GJ (2013) Direct visualization of "coagulative nucleation" in surfactant-free emulsion polymerization. Langmuir 29(37):11724–11729
32. Qin J, Zhang G, Shi X (2017) Study of a shear thickening fluid: the suspensions of monodisperse polystyrene microspheres in polyethylene glycol. J Dispers Sci Technol 38(7):935–942
33. Brown E, Forman NA, Orellana CS, Zhang H, Maynor BW, Betts DE, DeSimone JM, Jaeger HM (2010) Generality of shear thickening in dense suspensions. Nat Mater 9(3):220–224
34. Krieger IM, Dougherty TJ (1959) A mechanism for non-Newtonian flow in suspensions of rigid spheres. Trans Soc Rheol 3(1):137–152
35. Desiraju G (1998) Distinction between the weak hydrogen bond and the van der Waals interaction. Chem Commun 8:891–892
36. Steiner T (2002) The hydrogen bond in the solid state. Angew Chem Int Ed 41(1):48–76